JOURNAL OF GEOPHYSICAL RESEARCH, VOL. 104, NO. D24, PAGES 31,109-31,125, DECEMBER 27, 1999

# Diurnal and semidiurnal variations in global surface wind and divergence fields

Aiguo Dai and Clara Deser

National Center for Atmospheric Research, Boulder, Colorado

**Abstract.** Diurnal and semidiurnal variations in surface winds and wind divergence over the globe (50°S–70°N) are documented using 3-hourly wind observations from ~10,000 land stations and available marine reports during 1976-1997. A strong diurnal cycle in surface winds is found over land areas (strongest over high terrain and in summer) with an amplitude of 0.6–1.1 m/s for wind speed and 0.5–0.7 m/s for the zonal and meridional wind components. Surface wind speed peaks in the early afternoon over most of the globe. It is suggested that increased downward turbulent mixing of momentum during the day could be one of the main causes for the early afternoon maximum of surface wind speed. The diurnal anomalies of surface wind divergence tend to be out of phase in adjacent regions. In particular, land areas (except for extreme inland locations) exhibit maximum divergence around dawn (0600–0800 local solar time(LST)), while nearby oceanic regions have their maximum divergence in the evening (1700–1900 LST). Thus, there is evidence for a large-scale diurnal circulation in which surface air rises and converges over the continents and sinks and diverges over nearby oceans in the afternoon and early evening, and the opposite occurs in the early morning. Over the tropical Atlantic and Pacific Oceans (10°S–10°N), a zonally coherent pattern of maximum convergence (divergence) north (south) of the equator around 0900-1200 LST is generally similar to the latitudinal profile of the mean daily divergence, indicative of an enhancement of the local Hadley cell around 1030 LST relative to the daily mean. Another zonally coherent north-south dipole occurs over the North Pacific, with maximum surface wind divergence (convergence) around 0600–0800 LST in the subtropics (midlatitudes). This phase pattern correlates with cloud cover over the two regions. Over the United States, surface divergence peaks around 0600 LST in the west and the east and around 2000 LST in the center.

## 1. Introduction

Solar heating in the atmosphere, combined with other regional forcings, generates internal gravity waves in the atmosphere at periods of integral fractions of a solar day, especially at the diurnal and semidiurnal periods. These waves cause regular oscillations in atmospheric pressure, temperature, and wind fields which are often referred to as atmospheric tides [*Wallace and Hartranft*, 1969; *Chapman and Lindzen*, 1970; *Haurwitz and Cowley*, 1973; *Hsu and Hoskins*, 1989; *Whiteman and Bian*, 1996; *Dai and Wang*, 1999]. Although the tidal variations in winds are much larger in the upper atmosphere than at the surface [*Wallace and Hartranft*, 1969; *Williams and Avery*, 1996], large diurnal and semidiurnal variations in surface or lower tropospheric winds are found over tropical islands [*Aspliden*, 1977; *Williams et al.*, 1992], the open oceans in the tropical Pacific [*Gutzler and Hartten*, 1995; *Deser*, 1994; *Deser and Smith*, 1998] and tropical Atlantic [*Pedder*, 1978; *Nitta and Esbensen*, 1974], the central United States [*Hering and Borden*, 1962; *Reiter and Tang*, 1984], southern India [*Sivaramakrishnan et al.*, 1993], northeastern Australia [*May*, 1995], and eastern Africa [*Savijarvi*, 1997]. For example, *Heino* [1978] finds that diurnal variations of surface wind speed accounts for more than 50% of the total variance in summer over Finland. Over the tropical Pacific, *Deser and Smith* [1998] find that the semidiurnal cycle dominates the daily variation of the surface zonal wind component ($u$) with an average amplitude of 0.15 m/s and a phase (time of maximum, or $T_{\max}$) of 0310 and 1510 local solar time (LST), while the diurnal cycle dominates for the meridional wind component ($v$), which peaks around 0600–0900 (1800–2000) LST north (south) of the equator and has an average amplitude of 0.19 m/s.

Many of the features of daily wind variations documented by the above regional studies have been found to be related to local forcing such as solar heating asso-



Paper number 1999JD900927.
0148-0227/99/1999JD900927$09.00

ciated with topography, latent heating in moist convection, and differential solar heating over adjacent water and land surfaces. To separate the migrating, global tidal waves from the nonmigrating, regional tidal signals, one needs to analyze the daily variations on a global scale.

The daily variations in surface wind divergence have been documented only for limited regions in the tropical Atlantic [*Nitta and Esbensen*, 1974; *Pedder*, 1978; *Dewart*, 1978] and tropical Pacific [*Deser and Smith*, 1998], where diurnal variations in surface divergence appear to be out of phase between 5°N and 5°S. *Dai et al.* [1999] analyzed the diurnal variations of surface divergence associated with the diurnal and semidiurnal tides in surface pressure fields over the contiguous United States.

The diurnal cycle in low-level wind convergence may be related to that in precipitation. *Dai et al.* [1999] suggest that the diurnal cycle in low-level convergence over the United States largely controls the diurnal timing in summer precipitation (late afternoon maxima over the Rockies and the East and nocturnal maxima in the central United States). Limited ship observations suggests that maritime precipitation is significantly more frequent at night, with a maximum around 0300 LST over the northern (30°N–58°N) Atlantic and Pacific [*Kraus*, 1963]. Satellite and surface observations also show early morning or predawn maxima in tropical oceanic rainfall [*Janowiak et al.*, 1994; *Chang et al.*, 1995] and deep convection [*Gray and Jacobson*, 1977; *McGarry and Reed*, 1978; *Albright*, 1987; *Fu et al.*, 1990; *Hendon and Woodberry*, 1993]. However, a late afternoon maximum of convection was found over the tropical eastern Atlantic *Reed and Jaffe*, 1981].

Several complementary mechanisms have been proposed to explain the diurnal cycle in deep convective rainfall over the tropical oceans. These include day-night variations in tropospheric radiative cooling rates [*Gray and Jacobsen*, 1977; *Foltz and Gray*, 1979], cloud-radiation interactions [*Randall et al.*, 1991; *Xu and Randall*, 1995], and daytime heating of the sea surface *Hendon and Woodberry*, 1993; *Chen and Houze*, 1997]. However, the relative importance of these processes has not yet been resolved. Results of diurnal variations of surface winds and divergence should provide insights into the mechanisms for the diurnal cycle in the oceanic rainfall and convection.

In this study, we document the mean diurnal and semidiurnal variations in surface wind speed, zonal and meridional wind components, and surface wind divergence over the globe (50°S–70°N) by analyzing 3-hourly data from approximately 10,000 land and island stations and individual marine reports from the Comprehensive Ocean-Atmosphere Data Set (COADS) during 1976–1997. To the best of our knowledge, this work represents the first attempt to examine the mean daily variations of surface winds and wind divergence on a global basis. We also discuss the implications of our results in terms of causal mechanisms for the strong diurnal cycles in surface wind speed and wind divergence.

## 2. Data and Analysis Method

The 3-hourly station data of surface wind speed and direction, from which the zonal ($u$) and meridional ($v$) wind components are derived, were extracted from the Global Telecommunication System (GTS) synoptic weather reports archived at the National Center for Atmospheric Research (NCAR) (DS464.0, http://www.scd.ucar.edu/dss/datasets/ds464.0.html). This surface data set, which covers the time period from July 1976 to April 1997 and has a volume of about 2.5 GB per year, contains 3-hourly (0000, 0300, 0600 Coordinated Universal Time (UTC), etc.) surface wind measurements (typically made at about 10 meters above the ground) from about 15,000 land and island stations. We also processed the individual marine reports from the COADS data set [*Woodruff et al.*, 1993) from January 1976 to December 1995 (data after 1995 were not released at the time of our analysis). The COADS reports include hourly data from a small number of buoys in the equatorial Pacific, and 3-hourly data from ships and buoys. We used the COADS reports at the GTS 3-hourly reporting times.

Surface wind speeds are typically reported in units of knots (1 knot = 0.514 m/s). Although this precision is rather low compared to the diurnal amplitudes of surface winds, the averaging over a large number (up to 1800) of reports should substantially reduce the random errors in the measurements. While the winds are measured at a relatively stable height above the ground at the land and island stations, ships and buoys measure winds at various levels. The Tropical Atmosphere-Ocean (TAO) and other moored buoys measure winds at ~2 m above the sea surface. Anemometers on fishing and other small boats can be 2–20 m above the sea surface, while big commercial ships may measure winds at more than 20 m above the sea surface. The biases resulting from the variable measurement heights in marine surface wind data are discussed by *Kent et al.* [1993]. A preliminary evaluation suggested that ship-measured wind is as good a measure of the large-scale wind flow as the winds recorded at island stations [*Morrissey et al.*, 1988]. Despite their differences in the measuring height, winds measured by ships and buoys match fairly well [*Quayle*, 1984]. No attempts were made to adjust these biases in this study nor in COADS.

In contrast to land stations, which are fixed, the ship and many of the buoys are moving, and thus their reports are made at variable longitude/latitude locations. We averaged individual marine reports within each 2.5° longitude × 2° latitude box to obtain a mean value for each grid box at each reporting time. Land and fixed ocean stations were analyzed individually for the amplitude and phase of diurnal ($S_1$) and semidiurnal ($S_2$)

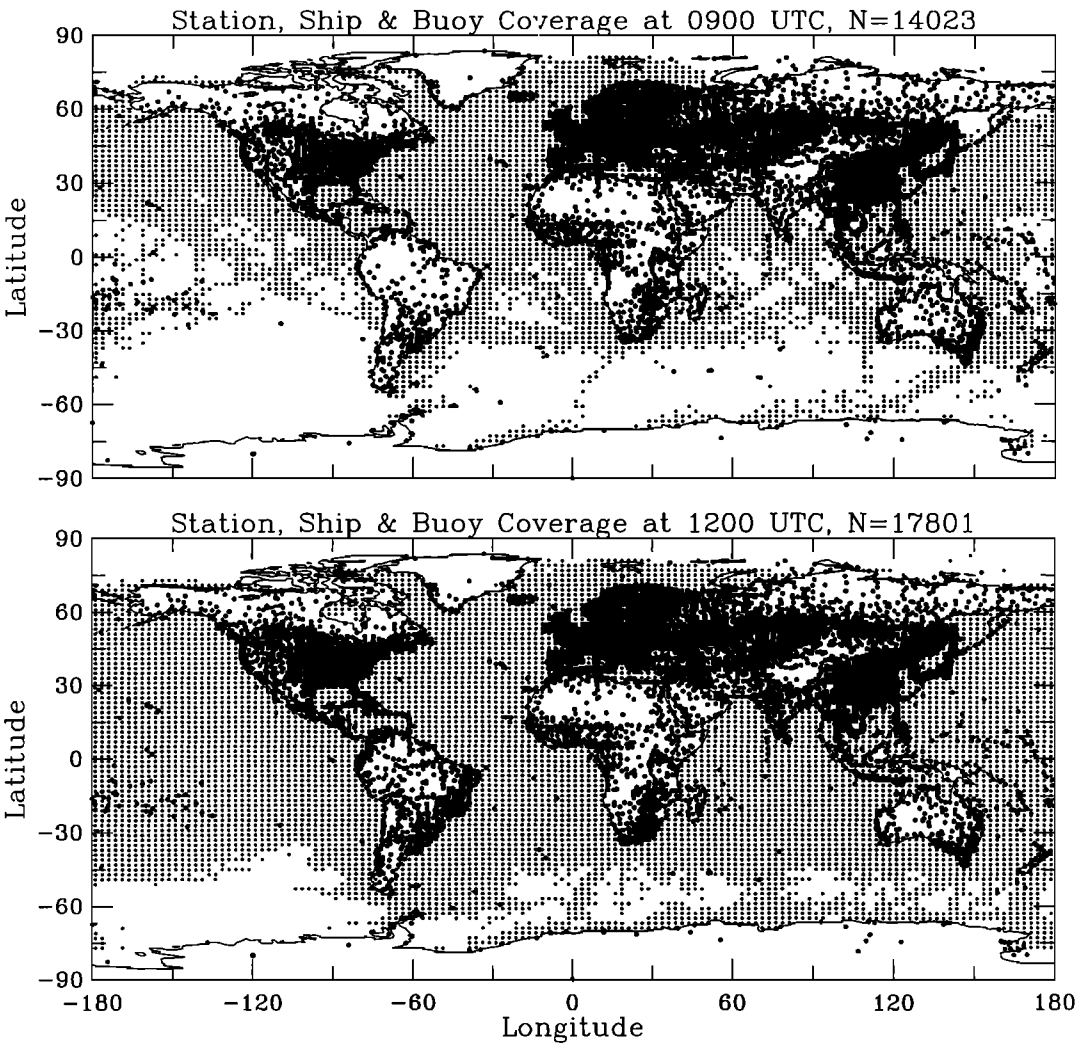


**Figure 1.** Stations (big dots) and 2.5° longitude × 2.0° latitude oceanic grid boxes (small dots) with 4 or more years of surface wind data during the 1976-1997 period at the 0900 UTC (top) and 1200 UTC (bottom) observation times. $N$ is the number of total stations and oceanic boxes.

harmonics which then were gridded onto a 2.5° longitude × 2° latitude grid using the natural neighbor interpolation method [*Watson*, 1992]. The gridded data of amplitude and phase were used in the spherical harmonic analysis.

The number of reports of surface winds at 0300, 0900, 1500 and 2100 UTC is generally smaller than at 0000, 0600, 1200, and 1800 UTC for both the GTS and COADS data sets (cf. Figure 1). Over much of the Southern Ocean (south of ~30°S) and parts of the equatorial Pacific, surface wind data are available only at 0000, 0600, 1200, and 1800 UTC. While these 6-hourly data are sufficient for sampling the diurnal harmonic, they are not adequate for capturing the semidiurnal cycle. Fortunately, the semidiurnal cycle of surface winds does not change rapidly in the longitudinal direction over the oceans [*Deser and Smith*, 1998]. Thus we were able to supplement the 6-hourly data at those oceanic grid boxes that have data only at 0000, 0600, 1200, and 1800 UTC (cf. Figure 1) by using reports (after daily mean is removed) 10° to the east (40 min later) and to the west (40 min earlier). This results in 12 reports per day (0000, 0040, 0520, 0600, 0640 UTC, etc.) at these oceanic boxes. Sampling tests with given diurnal and semidiurnal harmonics showed that the 3-hourly even sampling (i.e., 0000, 0300, 0600 UTC, etc.) and the supplemented 12 reports/day sampling are sufficient to exactly reproduce the original harmonics. Tests also showed that the supplementation of data points does not change the diurnal harmonics significantly.

The individual observations at each synoptic hour were averaged by season (DJF, December–February; MAM, March–May; JJA, June–August; and SON, September–November) for each year. For the seasonally averaged values to be used in our harmonic analysis we required at least 7 of the 8 synoptic hours having data for the land stations and 11 of the 12 supplemented synoptic hours having data for the oceanic

grid boxes. About 10,000 GTS stations and 5000–7000 ($2.5^o \times 2.0^o$) oceanic grid boxes meet this requirement with four or more years of data during the 1976-1997 period. GTS stations and oceanic grid boxes with less than four years of data were excluded in our analysis. The stations and oceanic grid boxes with sufficient data are shown in Figure 1 for the 0900 (similar for 0300, 1500, and 2100 ) UTC and 1200 (similar for 0000, 0600, 1800) UTC observation times. It can be seen that the station and marine observations provide good coverage over much of the globe except the Arctic Ocean, Greenland, the Antarctic, and the southern Pacific (south of $50^0$S) where the data are sparse. We shall focus on the region from 50°S to 70°N.

Surface divergence ($D = \nabla \bullet \mathbf{V}$, where $\mathbf{V}$ is horizontal wind vector) was computed (on sigma surface) using finite differencing from the observed $2.5^o$ longitude $\times$ $2.0^o$ latitude gridded winds. Tests showed that the finite-difference method yielded divergence fields similar to those derived using spectral methods.

The mean 3-hourly surface wind and divergence data ($Y$) at each location may be represented by

$$Y(t') = Y_0 + S_1(t') + S_2(t') + \text{residual} \qquad (1)$$

$$S_n(t') = A_n \sin(nt' + \sigma_n) = a_n \cos(nt') + b_n \sin(nt') \qquad (2)$$

where n=1, 2 (for diurnal and semidiurnal oscillations), $Y_0$ is the daily mean value, $S_1$ and $S_2$ are the diurnal and semidiurnal harmonics, respectively, $A_n$ is the amplitude (note that the peak-to-peak amplitude is $2A_n$), $\sigma_n$ is the phase, and $t'$ is mean local solar time (LST) expressed in degrees or radians (i.e., $t' = 2\pi t_1/24$, where $t_1$ is LST in hours). The residual in equation (1) contains the higher-order harmonics of the daily cycle which are not resolved by the 3-hourly sampling. Since previous analyses of hourly data showed that these high-frequency harmonics are much smaller than $S_1$ and $S_2$ over the tropical Pacific Ocean [*Deser and Smith*, 1998], the error induced by the aliasing of the high-frequency harmonics is likely to be small in equations (1) and (2).

A few examples of the fitted diurnal and semidiurnal oscillations of wind speed are shown in Figure 2. It should be emphasized that while the diurnal and semidiurnal harmonics can represent the diurnal variations reasonably well over majority of the locations, they fit the data poorly at some stations and ocean boxes, especially when the number of observations is small and/or the diurnal variations are weak. We shall use the percentage of the mean daily variance explained by the two harmonics as a measure of the goodness of fit.

The harmonic coefficients $a_n$ and $b_n$ are then interpolated onto a $2.5^o$ longitude $\times$ $2^o$ latitude grid using the natural neighbor interpolation method [*Watson*, 1992]. At each latitude, the gridded coefficients are then expanded using trigonometric series of the longitude so that the relative importance of various zonal modes with different wave numbers can be examined (see *Hau-*

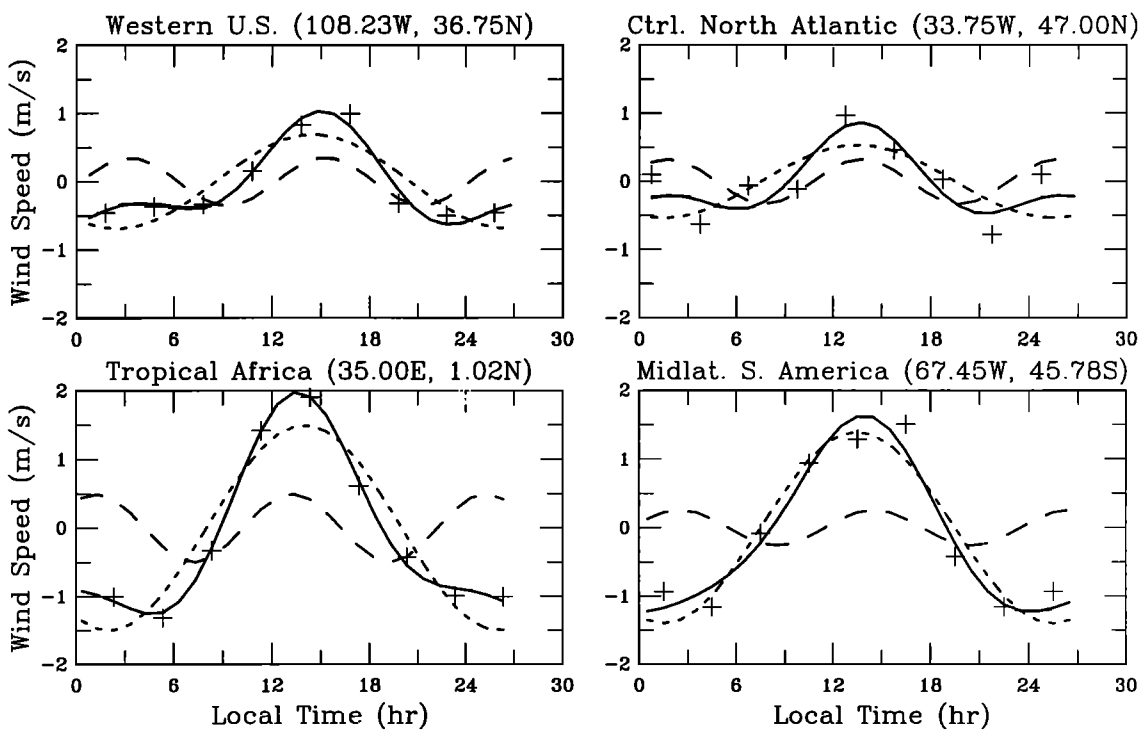


**Figure 2.** Observed mean DJF surface wind speed (pluses) together with the fitted diurnal (short-dashed curve) and semidiurnal (long-dashed curve) harmonics at four locations. The solid curve is the sum of the two harmonics.

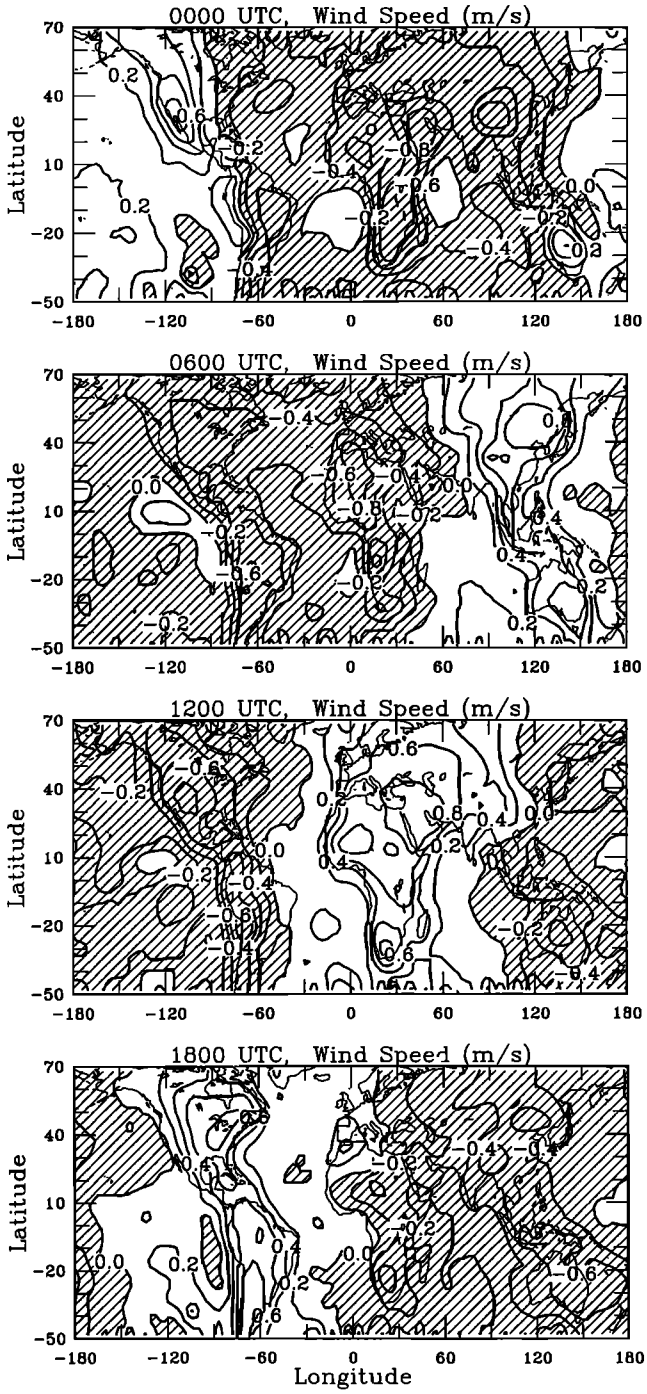


**Figure 3.** Annual mean surface wind speed anomalies (m/s) relative to the daily mean at the 6-hourly observation times derived by averaging and gridding the station and marine data of the 1976-1997 period. Negative values are hatched. Contour intervals are 0.2 m/s. Plots for seasonal means are similar.

*rwitz and Cowley* [1973] and *Dai and Wang* [1999] for details of the method).

The raw data of annual mean surface wind speed (expressed as departures from the daily mean) are shown in Figure 3 for the 6-hourly observation times. It can be seen that the westward propagating wave number 1 mode predominates. The dominant wave mode will become more clear in the zonal harmonic analysis of the data. Superposed on top of the migrating global mode, there are various regional features. For example, diurnal wind variations are larger over land than ocean and strongest over high terrain such as the Rocky Mountains, the Andes, and the Tibetan Plateau.

## 3. Results

### 3.1. Daily Variations of Surface Winds

Figure 4 shows the spatial distributions of the amplitudes of the diurnal and semidiurnal harmonics in annual mean wind speed, zonal, and meridional wind components averaged over the 1976-1997 period. It can be seen that the amplitudes of $S_1$ are generally larger over land (especially over high terrain such as the Tibetan Plateau and the western United States) than over ocean. It should be pointed out that large values over continental boundaries were interpolated onto adjacent oceans by the contouring package (same in Figure 5). The amplitude of $S_1$ for wind speed ranges from 0.6 to over 1.0 m/s over land areas. For the zonal and meridional wind components, the amplitudes of $S_1$ are about 0.3–0.4 m/s over the oceans and 0.5–0.7 m/s over middle- and low-latitude land areas. These are considerably smaller than those of wind speed, suggesting that diurnal variations in wind directions are relatively small. Analyses of wind direction data (not shown) indicate that the diurnal amplitude of wind direction is about 10° over the oceans and 10°-40° over land areas (larger in summer and over high terrains).

The semidiurnal harmonics in surface winds have an amplitude of about 0.2–0.3 m/s, which is substantially smaller than that of the diurnal harmonics (Figure 4). This is in contrast to surface pressure whose semidiurnal oscillation is stronger than or comparable to the diurnal oscillation over most of the globe [*Dai and Wang*, 1999]. There is also no significant land-sea difference in the amplitude of $S_2$ (consistent with the surface pressure field), suggesting that surface forcing of the semidiurnal oscillation is small.

Seasonal variations in the amplitudes of surface winds are significant only for $S_1$ and only over the land areas outside the tropics. Figure 5 shows that the amplitudes of $S_1$ of surface wind speed over North America and Eurasia vary from about 0.3–0.5 m/s in DJF to 0.7–1.1m/s in JJA. Similar seasonal variations are also seen for the zonal and meridional wind components (not shown).

Figure 6 shows the local solar time $T_{\max}$ when the diurnal harmonic peaks for annual mean wind speed. The diurnal harmonic of wind speed peaks around early afternoon (1400 LST) over most land areas and slightly earlier (1200–1400 LST) over the oceans. $T_{\max}$ over the Pacific off Mexico is in late afternoon (1600–1800 LST). This feature seems to be robust since there are

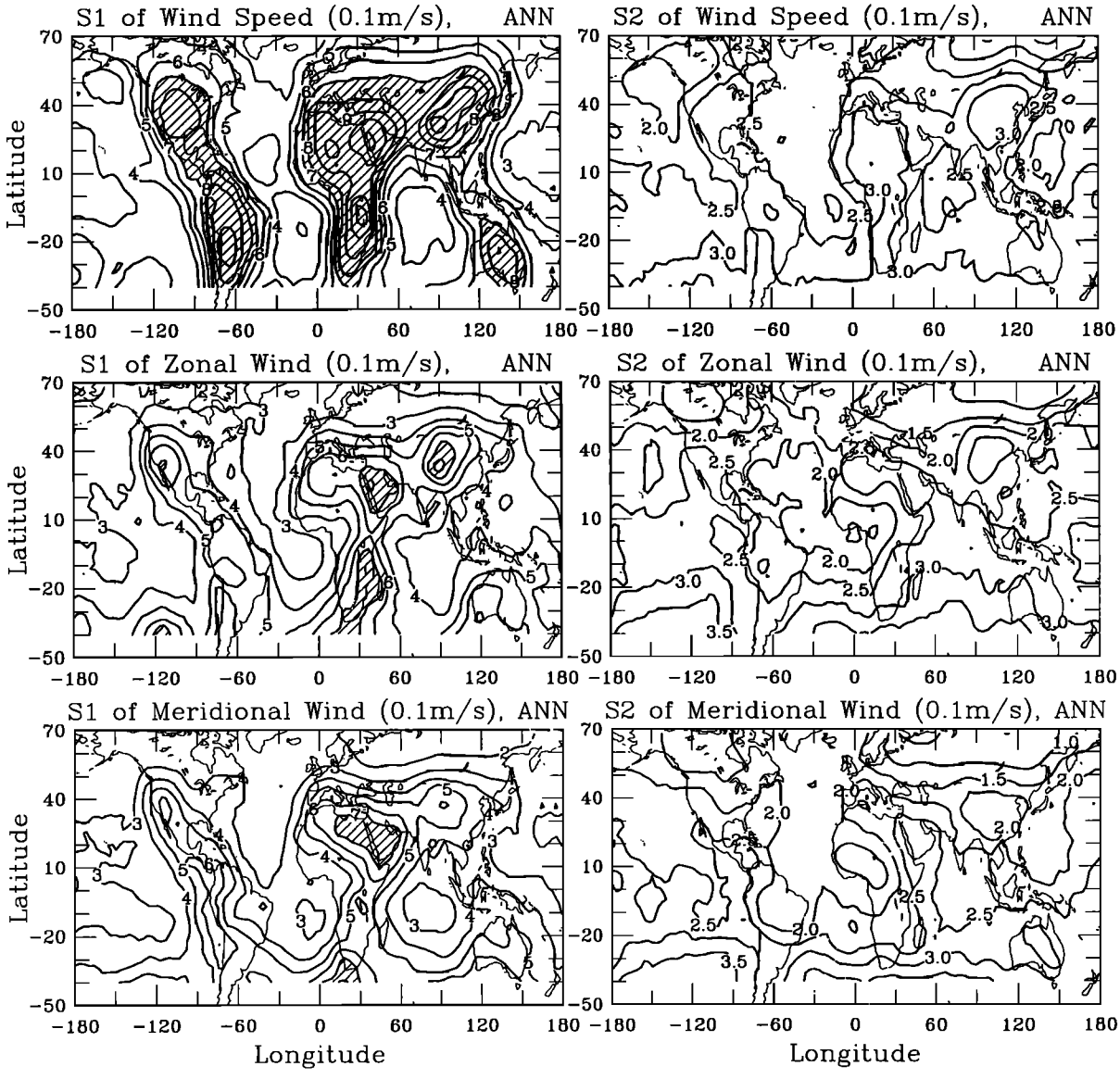


**Figure 4.** Amplitude (in units of 0.1m/s) of the diurnal ($S_1$, left column) and semidiurnal ($S_2$, right column) harmonics of mean annual surface wind speed (top panels), zonal (middle panels), and meridional (bottom panels) wind components. The amplitudes have been smoothed in space to reduce the small-scale noise. Contour intervals are 0.1 m/s for $S_1$ and 0.05 m/s for $S_2$. Values over 0.7 m/s are hatched.

sufficient ship reports from this area (cf. Figure 1). Compared with surface wind speed, the phase of the diurnal harmonics of the wind components (not shown) exhibits more regional variations, with $T_{\max}$ generally peaking around 1200 LST. The seasonal differences of $T_{\max}$ are generally small.

A convenient measure of the relative strengths of the diurnal and semidiurnal harmonics is the percentage of the mean daily variance accounted for (Figure 7). Over most land areas the diurnal (semidiurnal) harmonic explains 50–70% (10–20%) of the mean daily variance; while over the oceans, the percent variance explained is only slightly larger for the diurnal harmonic (30–40%) than for the semidiurnal harmonic (15–25%). Together, the two harmonics explain 60–90% of the mean daily variance over land areas and only about half of the daily variance over the oceans. This partly reflects the fact that the sampling errors are larger over ocean than over land.

### 3.2. Daily Variations of Surface Wind Divergence

To provide a context for diurnal variations in surface wind divergence, we show the daily mean surface wind and wind divergence fields for the annual mean, winter and summer (Figure 8). It can be seen that the Intertropical Convergence Zone (ITCZ) is well defined over the Pacific and Atlantic by the bands of maximum convergence (1.5–2.0 $\times$ $10^{-6}$ $s^{-1}$ for annual and DJF and 2–3 $\times$ $10^{-6}$ $s^{-1}$ for JJA). Over the Indian Ocean, the

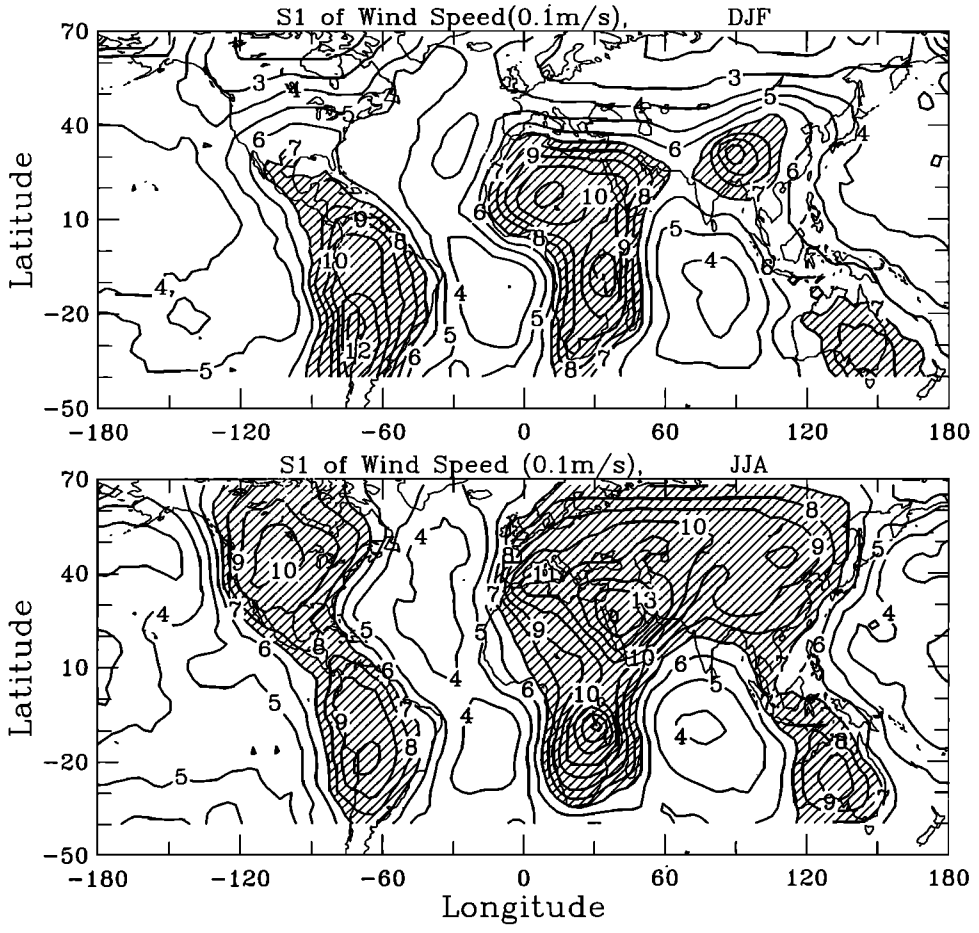


**Figure 5.** Same as Figure 4 ($S_1$ only) but for mean DJF (top) and JJA (bottom) surface wind speed.

tropical convergence zone spreads over a much wider region. The subtropical divergence centers over the oceans are close to the western boundaries of the continents and to the east of the centers of the subtropical pressure highs [e.g., *Shea*, 1986]. Strong divergence ($1.5–2.5 \times 10^{-6}$ s$^{-1}$) also occurs during DJF over the eastern coasts of Asia and North America where winds coming off the continents from the northwest accelerate over the oceans. Over North America, strong divergence occurs in the western and eastern parts of the continent, while convergence tends to occur in the middle. This pattern exists in all the seasons although the convergence in the middle is much reduced during DJF and extends farther to the west in JJA (the pattern in spring and autumn is very similar to that for the annual mean). The land (oceanic) areas tend to have more convergence (divergence) in summer (also see Figure 10) while the opposite is true in winter. This is no surprise because the boundary layer air over land is warmer than the air over ocean during summer, which leads to surface wind convergence and rising motion over land (vice versa in winter). We shall show that this mechanism may also explain the phase difference in the diurnal cycle of surface divergence between land and ocean.

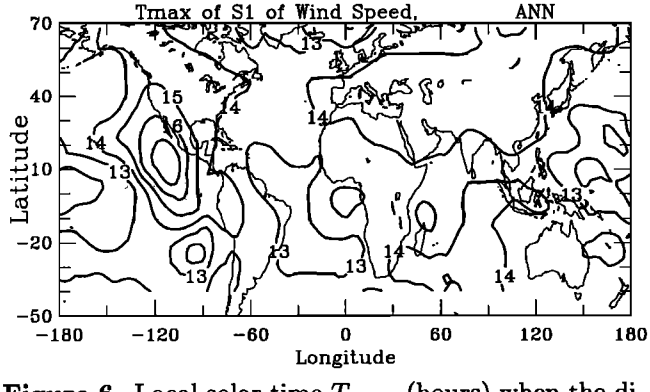


**Figure 6.** Local solar time $T_{max}$ (hours) when the diurnal harmonic ($S_1$) of annual mean surface wind speed peaks.

Figure 9 shows the amplitudes of the diurnal and semidiurnal harmonics of the annual mean, DJF and JJA divergence calculated from the observed winds. The diurnal amplitude of the divergence varies from 2.0 $\times 10^{-7}$ s$^{-1}$ over the oceans to about $3.0–5.5 \times 10^{-7}$ s$^{-1}$ over land areas. During boreal summer, maximum values occur over the western coast of North America, northern Africa, and the Middle East. During austral summer, the diurnal amplitude is largest ($4.0–5.5 \times 10^{-7}$ s$^{-1}$) over Australia and southern Africa. There

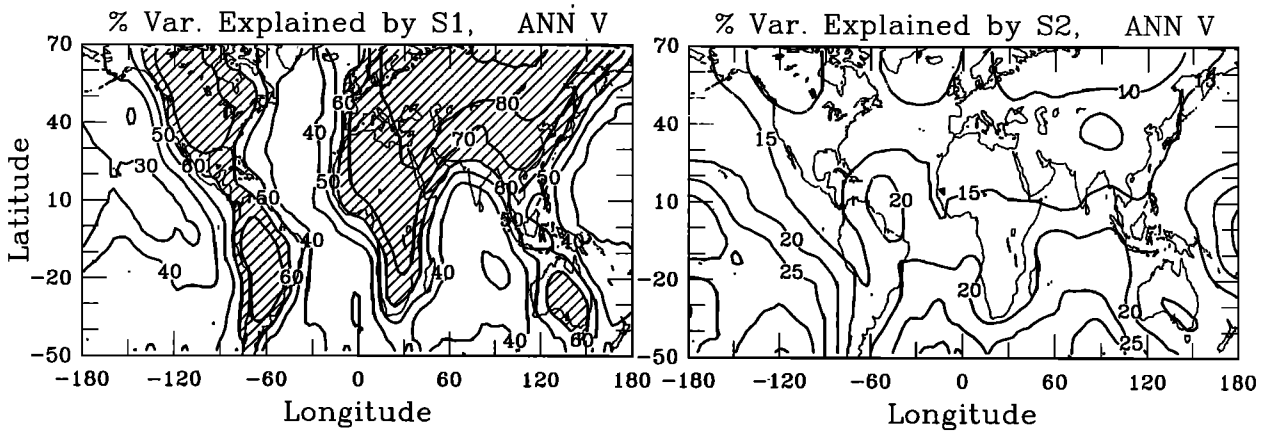


**Figure 7.** Percentage of the mean daily variance explained by the diurnal (left) and semidiurnal (right) harmonics of the annual mean surface wind speed. Plots for the zonal and meridional wind components are similar to those of wind speed.

are, however, no high values of the diurnal amplitude over the Bolivian highlands in DJF, which is likely due to the poor data sampling over the region (cf. Figure 1). The semidiurnal amplitude of the divergence is about $1.0-2.0 \times 10^{-7}$ s$^{-1}$ over most of the low and middle latitudes and does not vary much from winter to summer. The values at the higher latitudes (especially for $S_2$) are likely to have large uncertainties due to the limited number of observations there.

Plate 1 shows the $T_{\max}$ for annual mean surface wind divergence. The estimated phase may have large uncertainties (±1.5 hours), especially over the oceans. Nevertheless, some large-scale patterns are evident for many regions in Plate 1. It can be seen that the diurnal cycle of divergence tends to be approximately out of phase for many adjacent regions. For example, most land areas (except for the innermost parts of the continents) tend to have maximum divergence (or minimum convergence) around dawn (0600–0800 LST), while the oceans adjacent to the continents have maximum divergence in the evening (1700–1900 LST). This pattern is evident over almost all the continental boundaries, especially around Australia, North America, eastern Asia, the Indian subcontinent, and the Mediterranean Sea. Even though some innermost parts of Eurasia and North America do not follow this land-sea pattern, simple averaging (weighted by area) of the JJA divergence data over the land and oceanic areas between 25°N and 60°N results in two diurnal cycles with near opposite phases (Figure 10). Figure 10 also shows that the diurnal cycle dominates over the semidiurnal cycle over both the land and the oceanic areas at these northern latitudes. The above land-sea phase difference is most pronounced in summer but is also evident in other seasons and in the annual mean.

Over the United States the diurnal harmonic of surface divergence peaks around 0600 LST in the western and eastern United States and around 2000 LST in the central United States (Plate 1). This alternating feature, which is seen in all the seasons, resembles the pattern in the mean divergence field (Figure 8). Figure 11 (top) shows the mean daily march of surface divergence averaged over the western, central, and eastern United States during summer. The diurnal amplitude is largest ($9-12 \times 10^{-7}$ s$^{-1}$) in the western United States and smallest ($\sim 2 \times 10^{-7}$ s$^{-1}$) in the central United States. The diurnal cycle dominates over the semidiurnal cycle in the western and eastern United States. Figure 11 (bottom) shows the pattern of 1800 LST minus 0600 LST differences of surface winds and divergence. At 1800 LST relative to 0600 LST, strong winds (up to 2 m s$^{-1}$) from the Pacific (the Atlantic) and the Gulf of Mexico converge over the western (eastern) United States, while the wind anomalies are relatively weak over the central United States.

The phase map (Plate 1) of the diurnal harmonic of surface wind divergence shows a zonally coherent (although noisy) pattern within about 10° of the equator over the Pacific and Atlantic, with maximum convergence (divergence) north (south) of the equator around 0900–1200 LST. Accordingly, we zonally averaged the diurnal divergence anomalies across the eastern and central Pacific (180°–85°W) and Atlantic (55°W–15°E). Figure 12 shows the zonally averaged daily mean wind divergence profile, together with the zonally averaged divergence anomaly profile around 1030 LST for the Pacific (top) and Atlantic (bottom) domains in each season. Note that the scale for the daily mean divergence is in $10^{-6}$ s$^{-1}$, while the scale for the 1030 LST divergence anomaly is in $10^{-7}$ s$^{-1}$. With the exception of the Pacific in JJA the latitudinal structure of the divergence anomaly at 1030 LST is generally similar to the profile of the mean daily divergence, indicative of an enhancement (~10%) of the local Atlantic and Pacific Hadley cells at 1030 LST relative to the daily mean. In JJA over the Pacific the profile of anomalous divergence at

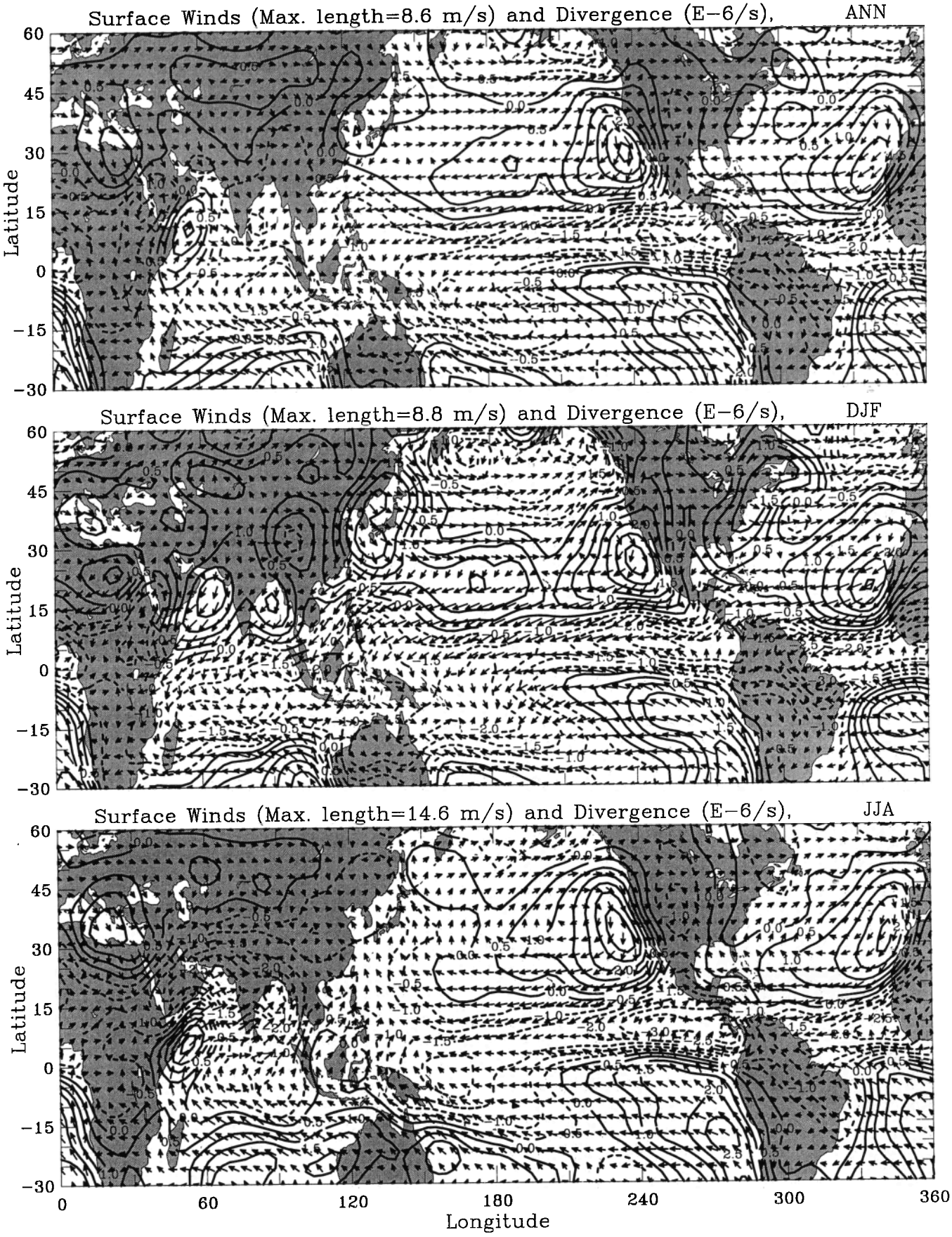


**Figure 8.** Observed (1976–1997) mean surface winds (arrows) and wind divergence ($10^{-6}$ $s^{-1}$, contours; dashed contours indicate convergence) calculated from the winds for the annual mean (top), DJF (middle), and JJA (bottom).

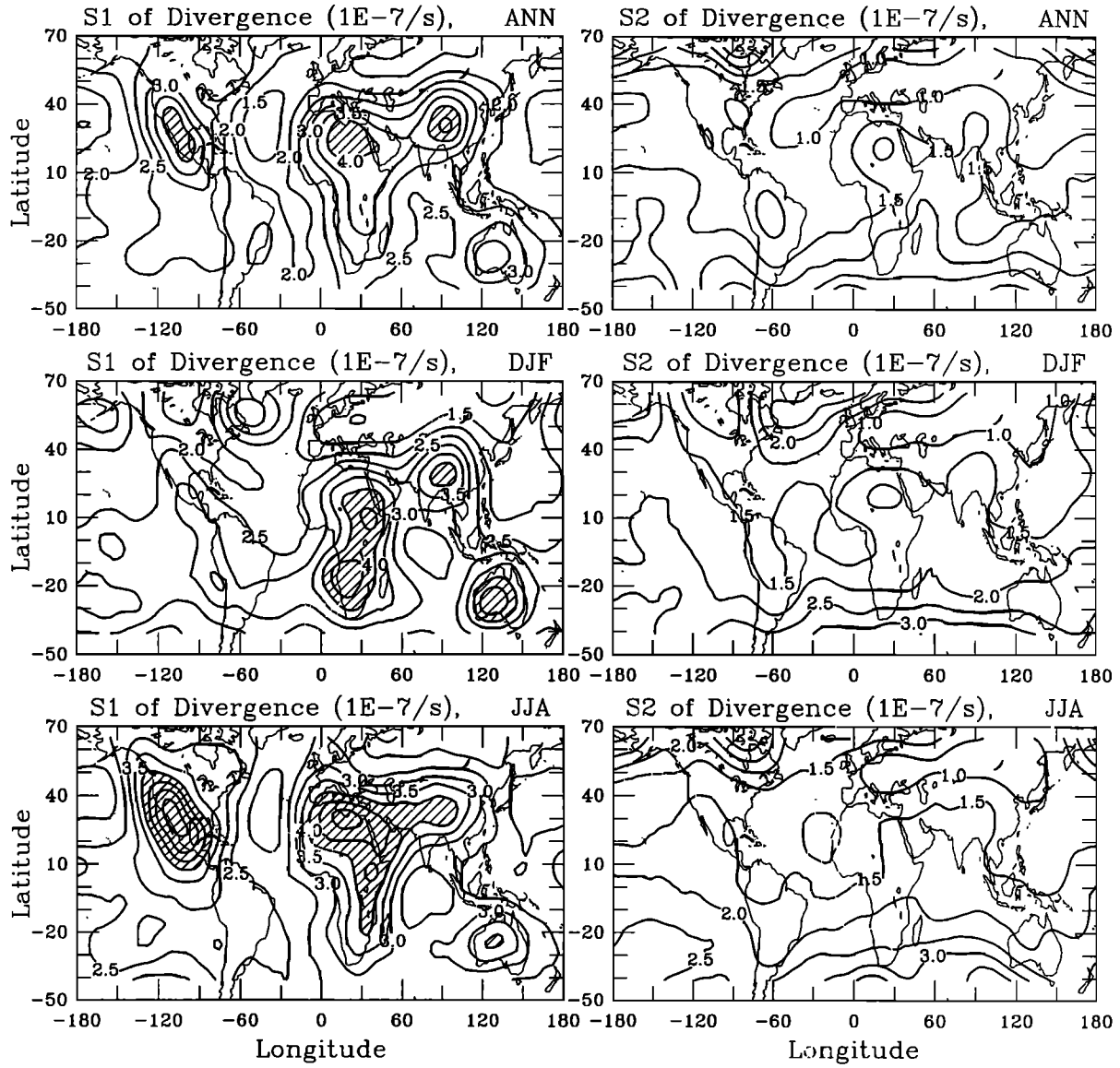


**Figure 9.** Same as Figure 4 but for annual mean, DJF and JJA surface divergence ($10^{-7}$ $s^{-1}$) calculated from the observed winds.

1030 LST is displaced southward by about 5° of latitude relative to the profile of daily mean divergence, and the strongest diurnal cycles are over the transition zones, not in the ITCZ. We do not understand the reasons for this displacement. The diurnal divergence results broadly support the findings of *Deser and Smith* [1998] for the tropical Pacific, although Deser and Smith found considerably larger amplitudes over the equatorial Pacific. This may be partly due to the higher temporal sampling (hourly data) and less smoothing in time and space in *Deser and Smith* [1998] than in the present study.

Figure 13 provides more detail on the diurnal variation of the local Hadley cell in the Atlantic during DJF. The surface divergence data confirm the phase pattern shown in Plate 1. Figure 13 shows that surface divergence over the equatorial Atlantic ITCZ (3.5°S−7.5°N) peaks around 0100 LST, which is out of phase with the regions to the north (7.5°N−19.5°N, $T_{max}\simeq$1300 LST) and south (3.5°S−18.5°S, $T_{max}\simeq$1400 LST). Compared with the Pacific ITCZ, where surface divergence peaks around 2230 LST, $T_{max}$ over the Atlantic ITCZ is 2−3 hours later. Our Atlantic ITCZ results are consistent with measurements made during the GARP Atlantic Tropical Experiment (GATE, about 5°N−10°N and 27°W−20°W): *Pedder* [1978] reports an amplitude of 0.2 × $10^{-6}$ $s^{-1}$ and a $T_{max}$ of 0310 LST, which is slightly later than that shown in Plate 1 and Figure 13.

The alternating pattern of divergence seen in the tropics also exists at higher latitudes over the central Pacific Ocean. Figure 14 shows the mean annual diurnal cycle of surface wind divergence zonally averaged

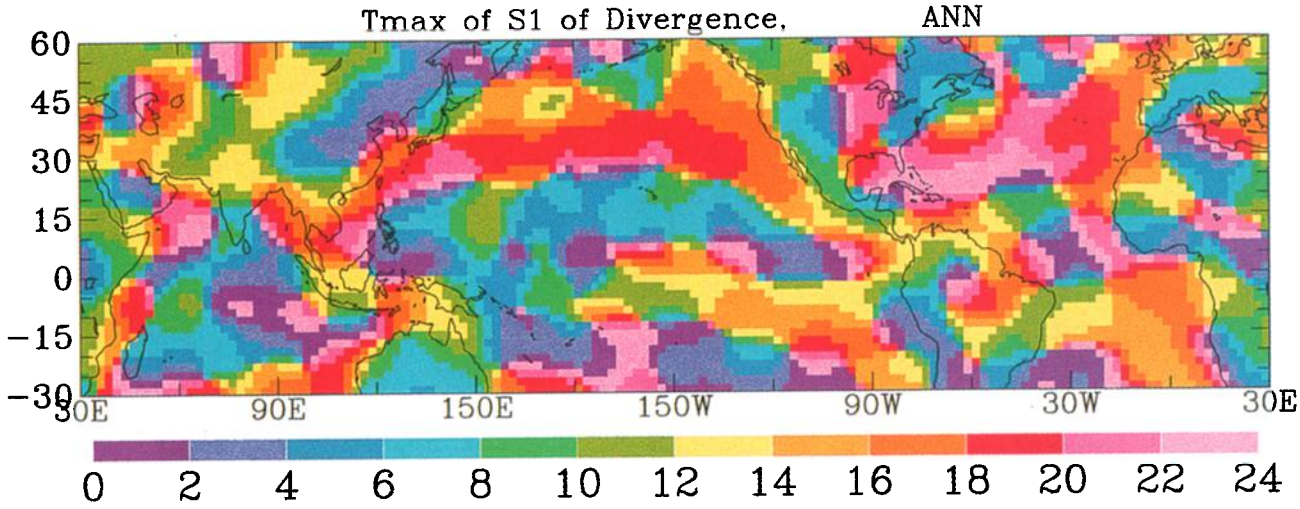


**Plate 1.** Same as Figure 6 but for surface wind divergence in colors.

across the central Pacific (160°E–130°W) as a function of latitude. It can be seen that the diurnal harmonic peaks around 1800–2000 LST from ~25°N to 42°N, which is out of phase with the region 10°–25°N. Across the equator the diurnal cycle is approximately out of phase between 0°–10°N ($T_{max}$=2100–2300 LST) and 0°–12°S ($T_{max}$=0900–1200 LST). The phase transition from 25°N to 12°S suggests that the diurnal cycle of surface divergence over the ITCZ (0°–10°N) is coupled with both the zones to the north (10°–25°N) and south (0°–12°S). Figure 14 also shows that the mean diurnal amplitude increases from about 0.5 × $10^{-7}$ $s^{-1}$ around the equator to 1.0–1.5 × $10^{-7}$ $s^{-1}$ in the subtropics in the Pacific. Over the South Pacific, $T_{max}$ is approximately 7 hours earlier over 12°S–28°S than over 0°–12°S. The amplitude over 12°S–28°S is also about twice that over the other latitudinal zones. Tests showed that the land stations within 12°S–28°S (cf. Figure 1) do not change the diurnal pattern in this zone. Over the Atlantic Ocean, the alternating pattern is also evident although strong coastal effects make it less pronounced than over the central Pacific Ocean (Plate 1).

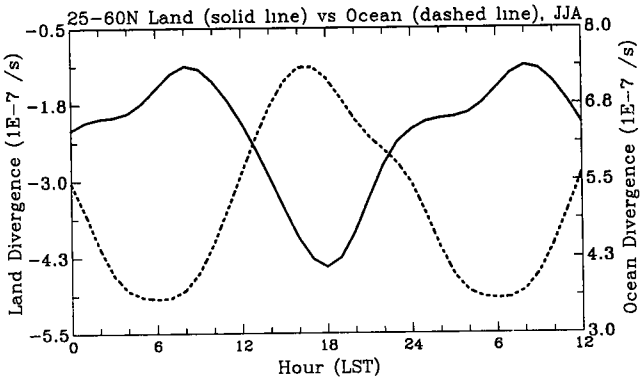


**Figure 10.** Mean surface wind divergence ($10^{-7}$ $s^{-1}$) during JJA averaged at each local time over the land (solid curve, left ordinate, negative values indicate convergence) and oceanic (dashed curve, right ordinate) areas from 25°N to 60°N.

### 3.3. Zonal Wave Components

The diurnal and semidiurnal oscillations can be expanded into various zonal wave components at each latitude. Figure 15 shows the globally (from 50°S to 70°N) averaged amplitudes for the important wave components of the annual diurnal and semidiurnal harmonics. The wave modes with positive (negative) wave numbers ($s$) travel toward the west (east), while the mode with $s$=0 is a standing wave. In particular, the wave with $s$=1 for $S_1$ ($s$ = 2 for $S_2$) travels westward at the speed of the mean Sun. When expressed in the local time, this wave is independent of the longitude and is called the migrating tide, whereas the other waves depends on both the local time and the longitude and are called nonmigrating tides [*Haurwitz and Cowley*, 1973].

Figure 15 shows that both the diurnal and semidiurnal oscillations are dominated by the migrating tides whose global mean amplitudes are about 5 times those of the nonmigrating tides. Contrary to surface pressure, whose global mean amplitude of the semidiurnal oscillation is greater than that of the diurnal oscillation [*Haurwitz and Cowley*, 1973; *Dai and Wang*, 1999], the global mean amplitudes of the diurnal oscillation of surface winds and divergence are larger than those of the semidiurnal oscillation, especially for their migrating components and for surface wind speed and divergence. This is consistent with the patterns shown in the raw data (Figure 3).

Globally averaged, the amplitudes of the two harmonics of the zonal wind component are only slightly larger than those of the respective harmonics of the meridional wind component. The diurnal harmonic of surface wind speed is about twice as strong as those of the wind components, while the semidiurnal harmonic of surface wind speed is considerably weaker than those

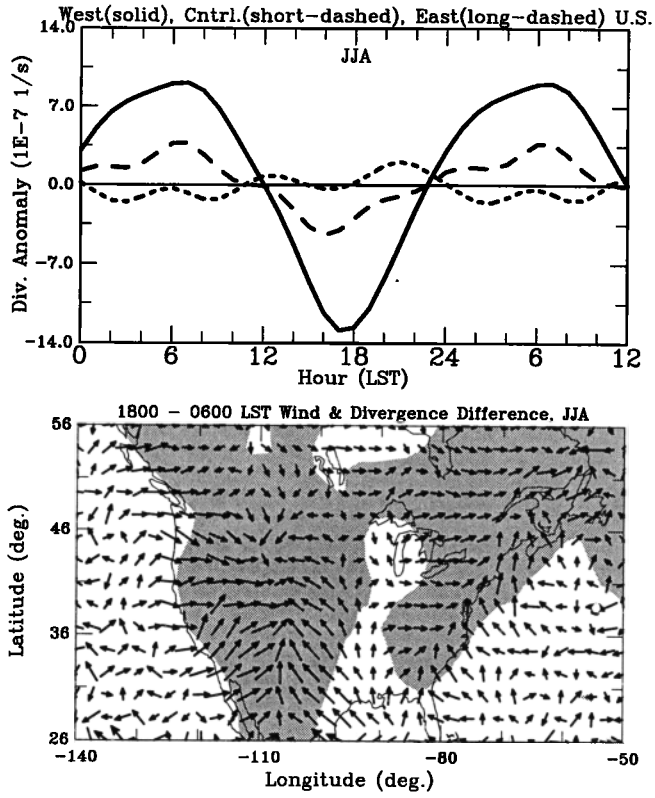


**Figure 11.** (top) Mean surface wind divergence anomalies($10^{-7}$ $s^{-1}$) during JJA averaged at each local time over the western (west of 100°W, solid curve), central (100°–85°W, short-dashed curve), and eastern (east of 85°W, long-dashed curve) United States. (bottom) Mean 1800 LST minus 0600 LST difference of surface winds (maximum arrow length = 2.0 m/s) and divergence (ranging from −1.0 to +0.5 × $10^{-5}$ $s^{-1}$, shaded (white) areas have negative (positive) divergence) for JJA over North America.

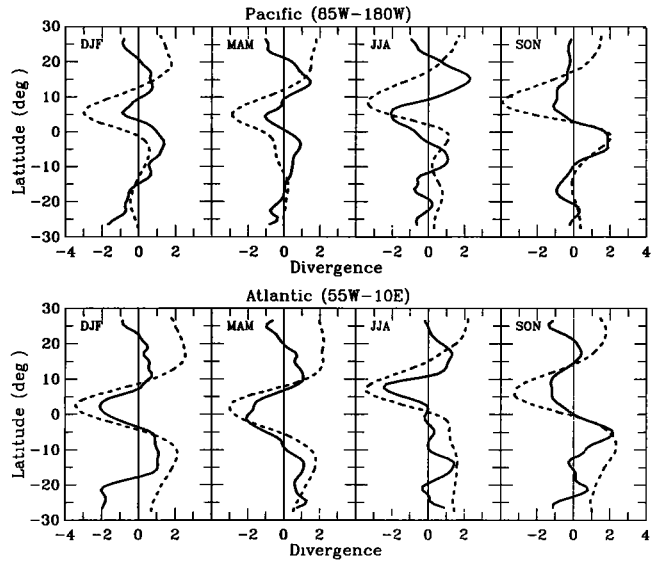


**Figure 12.** Mean seasonal surface divergence ($10^{-6}$ $s^{-1}$, dashed curve) and 1030 LST divergence anomaly (reconstructed from the diurnal harmonic) relative to the daily mean ($10^{-7}$ $s^{-1}$, solid curve) zonally averaged over the tropical Pacific from 85°W to 180°W (top) and the Atlantic from 55°W to 15°E (bottom).

of the wind components. Seasonal variations of the global mean amplitudes of the wave modes are small (not shown).

## 4. Discussion

The diurnal harmonic of wind speed (Figure 6) is approximately in phase with the diurnal cycle of surface air temperatures (Figure 16). Associated with higher surface temperatures during the day, sensible heat from the surface peaks in the afternoon, resulting in increased instability in the planetary boundary layer. This allows more downward turbulent mixing of momentum during the day than at night and contributes to the maximum wind speed in the afternoon. On the other hand, sensible heating from the surface can also generate spatial gradients in surface pressure fields and thus stronger winds during the day. The large land-sea difference in the amplitudes of $S_1$, which is also seen in the diurnal harmonic of surface pressure [*Dai and Wang*, 1999], is consistent with the stronger diurnal cycle in surface turbulent mixing and larger sensible heating over land

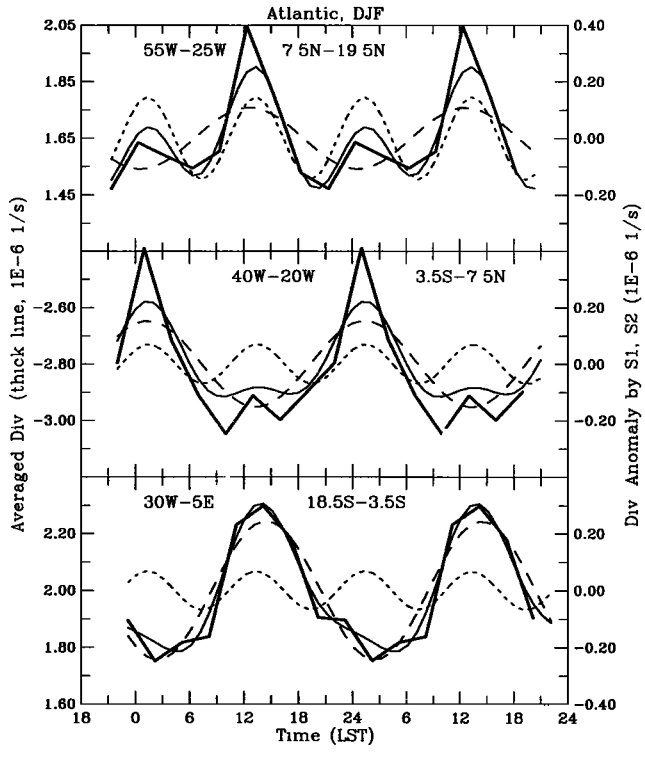


**Figure 13.** Diurnal evolution of the mean DJF divergence (thick solid curve) and divergence anomalies (relative to the daily mean) represented by the fitted diurnal (long-dashed curve) and semidiurnal (short-dashed curve) harmonics averaged over three latitudinal bands in the tropical Atlantic. The thin solid curve is the sum of the two harmonics. The averaging was done at each UTC time, but the results are plotted against the local time at the center of the zones as defined by the longitudes and latitudes indicated on each panel.

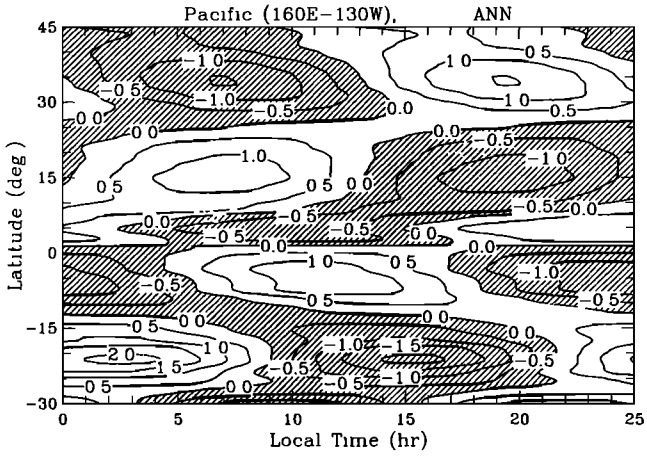


**Figure 14.** Annual mean diurnal cycle of the zonally averaged surface wind divergence ($10^{-7}$ $s^{-1}$) across the Pacific (160°E−130°W) as a function of latitude based on the estimated diurnal harmonic of the 1976-1995 period. The averaging was done at each local time. Positive (negative, hatched) values indicate divergence (convergence) relative to the daily mean.

than over ocean, although the same mechanisms may work over ocean as well.

The land-ocean phase differences in the diurnal cycle of surface wind divergence (Plate 1 and Figure 10) is analogous to the land-ocean differences in mean summer and winter divergence fields (cf. section 3.2 and Figure 8). During the daytime, land areas warm up more rapidly than the oceans, which results in much higher surface temperatures over land than over ocean in summer and the smallest land-ocean temperature difference in winter by the afternoon (1400−1600 LST) (Figure 16). During the night, radiative cooling decreases surface temperatures faster over land than over ocean, which results in substantially lower temperatures over land than over ocean in summer and the largest land-ocean temperature difference in winter around dawn (Figure 16). Associated with this diurnal cycle in the land-ocean difference of surface air temperatures, which is primarily due to land temperature changes, there should be a continental-scale diurnal atmospheric circulation (superposed on top of the daily mean circulation) in which surface air rises and converges over land areas and sinks and diverges over the oceans in the afternoon and early evening, and the opposite in the early morning. The land-ocean phase difference in the diurnal cycle of surface divergence is consistent with the existence of such a solar-driven diurnal circulation between the continents and the oceans with a mean amplitude of $\sim 2 \times 10^{-7}$ $s^{-1}$ (Figure 10).

Figure 11 shows that much of the air mass associated with the diurnal cycle of surface wind divergence over the western and eastern United States comes from the adjacent oceans (including the Gulf of Mexico) with a small contribution from the central United States. This suggests that the diurnal land-ocean circulation described above is a primary cause for the diurnal phase pattern of surface divergence over the western and eastern United States. *Dai et al.* [1999] suggest that this diurnal cycle of divergence could be a major factor controlling the diurnal timing of summer convective precipitation over the United States.

The diurnal cycle of surface convergence is generally consistent with the diurnal cycle of convective precipitation which tends to have a nighttime or an early morning maximum over many oceanic regions [*Kraus*, 1961; *Janowiak et al.*, 1994; *Chang et al.*, 1995] and a late afternoon maximum over land areas [*Dai et al.*, 1999]. However, Plate 1 shows that there are exceptions to this general tendency. For example, surface wind convergence occurs from about midnight to 1000 LST over the central United States (Figure 11) (which is roughly consistent with the early morning precipitation maximum there) and in the late afternoon and evening (1800-2100 LST) over the central Pacific from 10°N to 25°N (Figure 14).

Gray and colleagues [*Gray and Jacobsen*, 1977; *Foltz and Gray*, 1979] have suggested that low-level divergence (convergence) should be a maximum at the end of the night over relatively clear-sky (cloudy) areas due to the fact that atmospheric radiative cooling at night is larger over clear-sky than cloudy areas. The phase pattern of the diurnal harmonic of surface divergence over the central Pacific from 10°N−25°N to 25°N−45°N and over the equatorial ITCZ region is correlated with cloud cover over these regions (Figure 17) in a manner that appears to broadly support the radiative cooling hypothesis. However, the afternoon maximum in surface wind convergence over the southern Pacific convergence zone (~15°−27°S) seems to be inconsistent with the radiative cooling mechanism. Further study is needed to understand the diurnal phase differences in surface wind divergence between the North and the South Pacific.

Marine stratus cloud cover off the western boundaries of the subtropical Americas and Africa has been found to exhibit substantial diurnal variations (amplitude = 3−10%, strongest in summer), with maxima around 0300−0500 LST [*Warren et al.*, 1988; *Rozendaal et al.*, 1995]. It has been suggested that absorption of solar radiation within the clouds (which causes entrainment of dry air from above the boundary layer that dissipates the stratus during the day) and advection of moist boundary layer air from an upwind region more favorable to cloud formation could be responsible for the early morning maximum of marine stratus clouds [*Rozendaal et al.*, 1995]. Plate 1 shows that the diurnal maximum of convergence (divergence) is in phase with the early morning maximum (late afternoon minimum) of stratus clouds over the above regions. Since surface convergence (with a diurnal amplitude of $\sim 3-4 \times 10^{-7}$ $s^{-1}$) enhances the moisture flux into the marine boundary layer, it may favor stratus cloud formation. The relative importance of diurnal convergence versus diurnal cloud top heating for the observed diurnal cycle of marine stratus clouds remains to be assessed.

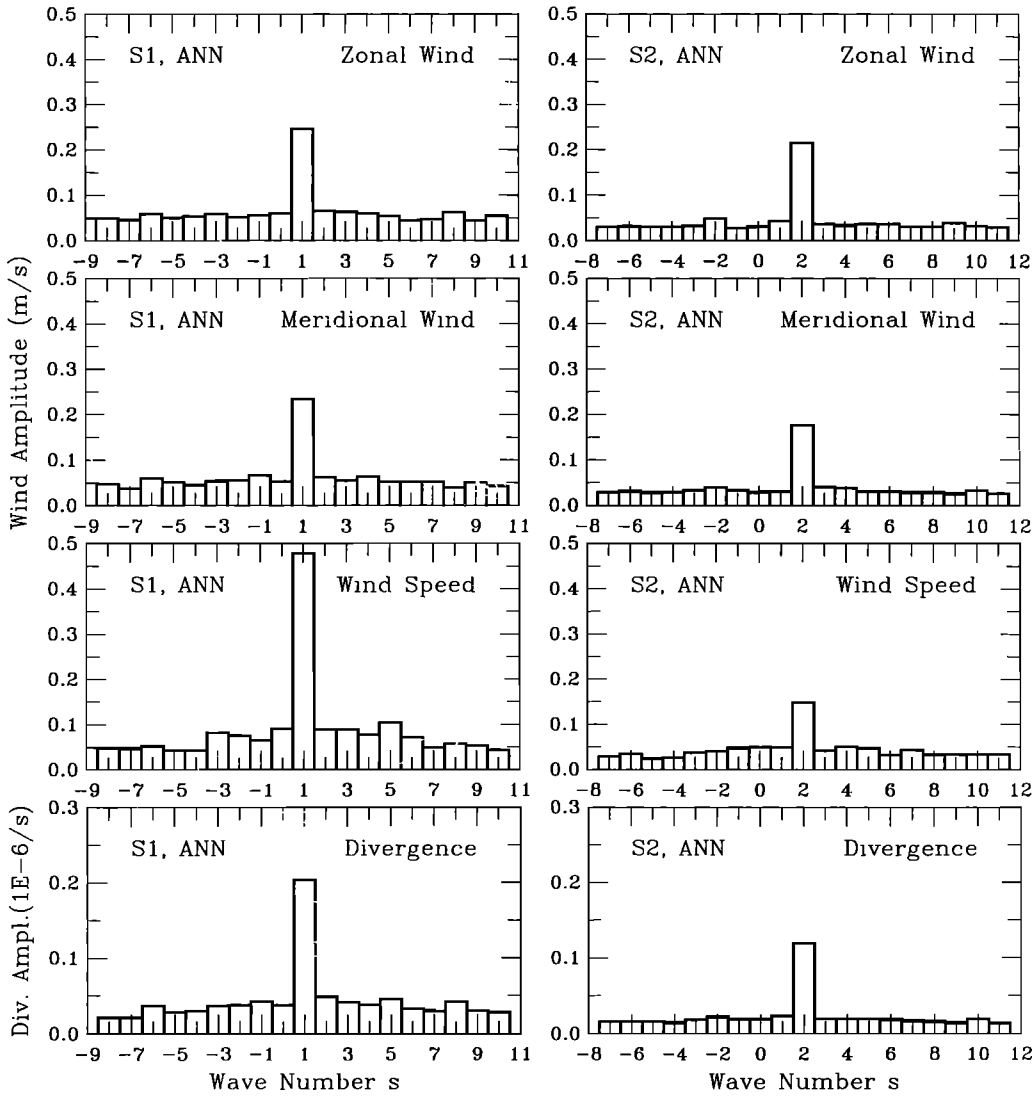


**Figure 15.** Globally (50°S–70°N) averaged amplitudes of the diurnal (left column) and semidiurnal (right column) cycles at various zonal wave numbers for mean annual surface wind components, wind speed, and divergence.

## 5. Summary

Diurnal and semidiurnal variations in surface winds and wind divergence over the globe (50°S–70°N) have been documented using 3-hourly wind observations from approximately 10,000 stations and COADS marine reports during 1976-1997. The main results are summarized as follows:

Surface winds have a strong diurnal cycle over land areas (strongest over high terrain such as the Tibetan Plateau, the western United States, and the Andes and in summer) with an amplitude of 0.6–1.1 m/s for wind speed and 0.5–0.7 m/s for the zonal and meridional wind components. Over the oceans the amplitude of the diurnal cycles is about 0.3–0.4 m/s for both the wind speed and the wind components and vary little from winter to summer. The semidiurnal cycle in surface winds is weaker than the diurnal cycle and has an amplitude of 0.2–0.3 m/s over both land and ocean for wind speed and the wind components in all the seasons. The diurnal cycle accounts for 50–70% of the daily variance over land and 30–40% of the daily variance over ocean, while the semidiurnal cycle explains about 15–25% of the daily variance over most of the globe.

The diurnal harmonic of surface wind speed peaks around early afternoon (1400 LST) over most land areas and around 1200–1400 LST over the oceans, which is approximately in phase with the diurnal cycle of surface air temperatures. It is suggested that the increased downward turbulent mixing of momentum in the afternoon, which results from increased instability of the planetary boundary layer due to solar heating at the surface, could be a major mechanism for the diurnal cycle of wind speed; tidal variations in surface pressure and temperature could also contribute to the diurnal cycle of surface winds (largely over land).

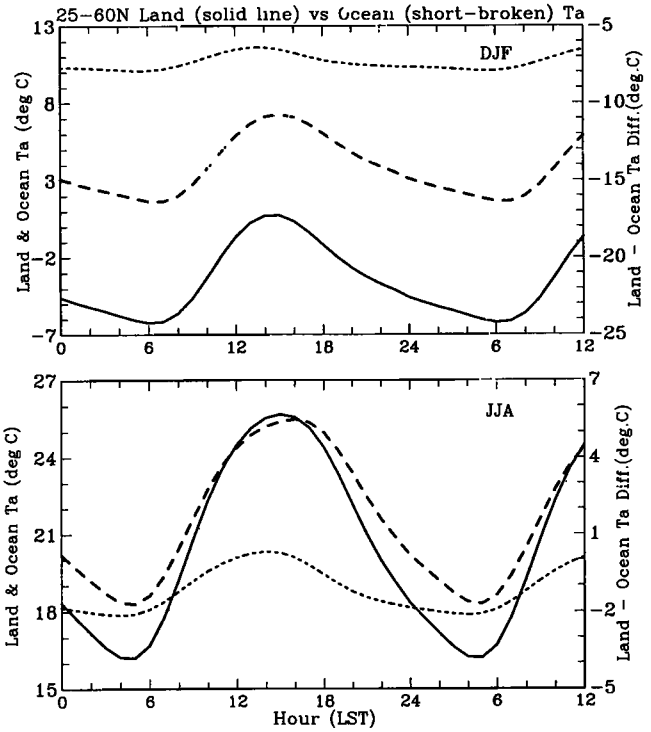


**Figure 16.** Observed mean surface air temperature (°C) during DJF (top) and JJA (bottom) averaged at each local time over the land (solid curve) and oceanic (short-dashed curve) areas from 25°N to 60°N. The long-dashed curve is the land minus ocean difference of surface air temperature (on the right ordinate). The temperature data are from the same data sets as for surface winds and have a coverage similar to Figure 1.

Surface wind divergence also has a stronger diurnal cycle over land, especially over high terrain and during summer, than over ocean, with an amplitude ranging from $2.0 \times 10^{-7}$ $s^{-1}$ over ocean to about $3.0–5.5 \times 10^{-7}$ $s^{-1}$ over land. The semidiurnal cycle has an amplitude of $1.0–2.0 \times 10^{-7}$ $s^{-1}$ over both land and ocean in all the seasons. The percentages of the daily variance explained by the two harmonics are comparable to those for surface winds.

The diurnal cycle of surface divergence tends to be out of phase for many adjacent regions. In general, land areas (except for the innermost parts of the continents) such as Australia, eastern Asia, western and eastern North America, the Indian subcontinent, and the Mediterranean region tend to have maximum divergence (minimum convergence) around dawn (0600–0800 LST), while the oceans adjacent to the continents have maximum divergence in the evening (1700–1900 LST). This suggests that there exists a continental-scale diurnal circulation superposed on top of the daily mean circulation in which surface air rises and converges over the continents and sinks and diverges over the adjacent oceans in the afternoon and early evening, and the opposite occurs in the early morning. The land-ocean phase difference of surface divergence is also consistent with the notion that precipitation tends to peak at night over the oceans and in the afternoon over most land areas.

Surface wind divergence peaks around 0600 LST in the western and eastern United States and around 2000 LST in the central United States. This alternating feature is evident in all the seasons and resembles the pattern in the mean divergence field. It is also consistent with the phase changes across the United States in summer precipitation [*Dai et al.*, 1999].

Over the central Pacific, the diurnal anomaly of surface wind divergence peaks around 0600–0800 LST from 10°N to 25°N and about 12 hours later from 25°N to 45°N. This phase pattern is correlated with cloud cover in a manner that is consistent with the radiative cooling hypothesis [*Gray and Jacobsen*, 1977; *Foltz and Gray*, 1979] for the diurnal cycle in oceanic rainfall and convection.

Over the tropical Atlantic and eastern and central portions of the tropical Pacific, there exists a zonally coherent pattern with maximum convergence (divergence) north (south) of the equator around 0900–1200 LST. With the exception of the Pacific in JJA, the latitudinal structure of the divergence anomaly at 1030 LST is generally similar to the profile of the mean daily divergence, indicative of an enhancement (~10%) of the local Atlantic and Pacific Hadley cells at 1030 LST relative to the daily mean.

Diurnal anomalies tend to be convergent (divergent) in the early morning (late afternoon to evening) over subtropical oceanic regions off the western boundaries of Americas and Africa. This is in phase with the diurnal cycle of stratus cloud cover over these regions. It is suggested that the diurnal cycle of large-scale divergence may contribute to the diurnal variations of marine stratus cloud cover.

The daily anomaly of surface wind speed is dominated by westward propagating wave number 1 mode, which is the main zonal wave of the diurnal harmonic. For the zonal and meridional wind components and surface wind divergence, both the wave number 1 mode of the diurnal harmonic and the wave number 2 mode of

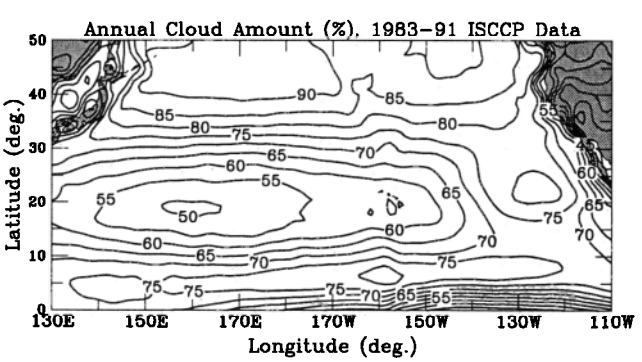


**Figure 17.** Satellite-observed mean (1983-1991) annual total cloud amount (%) over the northern Pacific derived from the International Satellite Cloud Climatology Project (ISCCP) data sets [*Rossow and Schiffer*, 1991].

the semidiurnal harmonic are important, although zonal wave components (except for wave number 2) of the diurnal harmonic are generally stronger than those of the semidiurnal harmonic.

The results of this study, especially those concerning the phase of surface wind divergence over the tropical Pacific and Southern Oceans, may contain large uncertainties due to the poor sampling of data. The exact range of the uncertainties is difficult to obtain because of the variable sampling resolution and number of reports. A value of $\pm 1.5$ hours (i.e., half of the sampling interval) may be used as a rough estimate for the error in the phase discussed above. Future enhancements to the data sets (e.g., COADS is updating the data set for the 1990s to include more hourly data from TAO buoys) should improve the results presented here. Analyses of the vertical structure of the diurnal variations of winds [*Pedder*, 1978; *Whiteman and Bian*, 1996; *Williams and Avery*, 1996] and divergence in the troposphere should provide a more complete picture of the surface diurnal circulations documented here.

**Acknowledgments.** We thank J. M. Wallace and two anonymous reviewers for their helpful comments. We are grateful to Steve Worley for assisting us with the COADS data set, Gregg Walters for his help with the GTS station data set, and Dennis Shea for computer assistance. A. Dai was supported by a NOAA Postdoctoral Program in Climate and Global Change fellowship, administered by the University Corporation for Atmospheric Research. The National Center for Atmospheric Research is sponsored by the National Science Foundation.

## References

Albright, M. D., Diurnal variation of deep convection and inferred precipitation in the central tropical Pacific during January-February 1979, *Mon. Weather Rev., 113*, 1663-1680, 1987.

Aspliden, C. I., Diurnal and semidiurnal low-level wind cycles over a tropical island, *Boundary-Layer Meteorol., 12*, 187-199, 1977

Chang, A. T. C., L. S. Chiu, and G. Yang, Diurnal cycle of oceanic precipitation from SSM/I data, *Mon. Weather Rev., 123*, 3371-3380, 1995.

Chapman, S., and R. S. Lindzen, *Atmospheric Tides*, D. Reidel, Norwell, Mass., 200 pp., 1970.

Chen, S. S., and R. A. Houze, Diurnal variation and lifecycle of deep convective systems over the tropical Pacific warm pool, *Q. J. R. Meteorol. Soc., 123*, 357-388, 1997.

Dai, A., F. Giorgi, and K. E. Trenberth, Observed and model simulated precipitation diurnal cycle over the contiguous United States, *J. Geophys. Res., 104*, 6377-6402, 1999.

Dai, A., and J. Wang, Diurnal and semidiurnal tides in global surface pressure fields, *J. Atmos. Sci., 56*, 3874-3891, 1999.

Deser, C., Daily surface wind variations over the equatorial Pacific Ocean, *J. Geophys. Res., 99*, 23,071-23,078, 1994.

Deser, C., and C. A. Smith, Diurnal and semidiurnal variations of the surface wind field over the tropical Pacific Ocean, *J. Clim., 11*, 1730-1748, 1998.

Dewart, J. M., Diurnal variability in the GATE region, *Atmos. Sci. Pap. 298*, Dept. of Atmos. Sci., Colorado State Univ., Fort Collins, 1978.

Foltz, G. S., and W. M. Gray, Diurnal variation in the troposphere's energy balance, *J. Atmos. Sci., 36*, 1450-1466, 1979.

Fu, R., A. D. DelGenio, and W. B. Rossow, Behavior of deep convective clouds in the tropical Pacific from ISCCP radiances, *J. Clim., 3*, 1129-1152, 1990.

Gray, W. M., and R. W. Jacobson, Jr., Diurnal variation of deep cumulus convection, *Mon. Weather Rev., 105*, 1171-1188, 1977.

Gutzler, D. S., and L. M. Hartten, Daily variability of lower tropospheric winds over the tropical western Pacific, *J. Geophys. Res., 100*, 22,999-23,008, 1995.

Haurwitz, B., and D. Cowley, The diurnal and semidiurnal barometric oscillations, global distribution and annual variation, *Pure Appl. Geophys., 102*, 193-222, 1973.

Heino, R., On the diurnal variation of wind in Finland, *Tech. Rep. 17*, 21 pp., Finland Meteorol. Inst., Helsinki, 1978.

Hendon, H. H., and K. Woodberry, The diurnal cycle of tropical convection, *J. Geophys. Res., 98*, 16,623-16,637.

Hering, W. S. and T. R. Borden Jr., Diurnal variations in the summer wind field over the central United States, *J. Atmos. Sci., 19*, 81-86, 1962.

Hsu, H.-H., and B. Hoskins, Tidal fluctuations as seen in ECMWF data, *Q. J. R. Meteorol. Soc., 115*, 247-264, 1989.

Janowiak, J. E., P. A. Arkin, and M. Morrissey, An examination of the diurnal cycle in oceanic tropical rainfall using satellite and in situ data, *Mon. Weather Rev., 122*, 2296-2311, 1994.

Kraus, E. B., The diurnal precipitation change over the sea, *J. Atmos. Sci., 20*, 551-556, 1963.

Kent, E., P. K. Taylor, B. S. Truscott, and J. S. Hopkins, The accuracy of voluntary observing ships' meteorological observations – results of the VSOP-NA, *J. Atmos. Oceanic Technol., 10*, 591-608, 1993.

May, P. T., The Australian nocturnal jet and diurnal variations of boundary-layer winds over Mt. Isa in northeastern Australia, *Q. J. R. Meteorol. Soc., 121*(A), 987-1003, 1995.

McGary, M. M., and R. J. Reed, Diurnal variations in convective activity and precipitation during phases II and III of GATE, *Mon. Weather Rev., 106*, 101-113, 1978.

Morrissey, M. L., M. A. Lander, and J. A. Maliekal, Preliminary evaluation of ship data in the equatorial western Pacific, *J. Atmos. Oceanic Technol., 5*, 251-258, 1988.

Nitta, T., and S. Esbenson, Diurnal variations in the western Atlantic trades during BOMEX, *J. Meteorol. Soc. Japan, 52*, 254-257, 1974.

Pedder, M. A., Diurnal and semidiurnal variations in the A/B scale averaged wind fields during phase III of GATE, *Mon. Weather Rev., 106*, 782-788, 1978.

Quayle, R. G., Comparisons between ship and buoy climatologies, *Mar. Weather Log, 28*, 137-140, 1984.

Randall, D. A., Harshvardhan, and D. A. Dazlich, Diurnal variability of the hydrologic cycle in a general circulation model, *J. Atmos. Sci., 48*, 40-62, 1991.

Reed, R. J., and K. D. Jaffe, Diurnal variation of summer convection over West Africa and the tropical eastern Atlantic during 1974 and 1978, *Mon. Weather Rev., 109*, 2527-2534, 1981.

Reiter, E. R., and M. Tang, Plateau effects on diurnal circulation patterns, *Mon. Weather Rev., 112*, 638-651, 1984.

Rosendaal, M. A., C. B. Leovy, and S. A. Klein, An observational study of diurnal variations of marine stratiform cloud, *J. Clim., 8*, 1795-1809, 1995.

Rossow, W. B. and R. A. Schiffer, ISCCP cloud data products, *Bull. Am. Meteorol. Soc., 72*, 2-20, 1991.

Savijarvi, H., Diurnal winds around Lake Tanganyika, *Q. J. R. Meteorol. Soc., 123*, 901-918, 1997.

Shea, D. J., *Climatological Atlas: 1950-1979*, NCAR Tech. Note, NCAR TN-269+STR, 35 pp., 1986. (Available from Natl. Cent. for Atmos. Res., Boulder, Colo.)

Sivaramakrishnan, T. R., G. V. Rama, P. S. Prakash Rao, and K. Prakasam, Diurnal wind variation in the planetary boundary layer (PBL) over Sriharikota, India, *Boundary Layer, Meteorol., 63*, 197-204, 1993.

Wallace, J. M., and F. R. Hartranft, Diurnal wind variations, surface to 30 kilometers, *Mon. Weather Rev., 97*, 446-455, 1969.

Warren, S. G., C. J. Hahn, J. London, R. M. Chervin and R. L. Jenne, Global distribution of total cloud cover and cloud type amounts over the ocean. *NCAR Tech. Note, NCAR/TN-317+STR*, 42 pp., plus 170 maps, 1988. (Available from Natl. Cent. for Atmos. Res., Boulder, Colo.)

Watson, D. F., Contouring: A Guide to the Analysis and Display of Spatial Data, in *Computer Methods in the Geosciences*, vol. 10, 340 pp., Pergamon, New York, 1992.

Whiteman, C. D., and X. Bian, Solar semidiurnal tides in the troposphere: Detection by radar profiles, *Bull. Am. Meteorol. Soc., 77*, 529-542, 1996.

Williams, C. R., and S. K. Avery, Diurnal winds observed in the tropical troposphere using 50 MHz wind profilers, *J. Geophys. Res., 101*, 15,051-15,060, 1996.

Williams, C. R., S. K. Avery, J. R. McAfee, and K. S. Gage, Comparison of observed diurnal and semidiurnal tropospheric winds at Christmas Island with tidal theory, *Geophys. Res. Lett., 19*, 1471-1474, 1992.

Woodruff, S. D., S. J. Lubker, K. Wolter, S. J. Worley, and J. D. Elms, Comprehensive ocean-atmosphere data set (COADS) release 1a: 1980-1992, *Earth Sys. Monit., 4*(1), 1-8, 1993.

Xu, K., and D. A. Randall, Impact of interactive radiative transfer on the macroscopic behavior of cumulus ensembles, Part II, Mechanisms for cloud-radiative interactions, *J. Atmos. Sci., 52*, 800-817, 1995.

A. Dai and C. Deser, National Center for Atmospheric Research, P.O. Box 3000, Boulder, CO 80307. (e-mail: adai@ucar.edu; cdeser@ucar.edu)

(Received March 11, 1999; revised August 10, 1999; accepted August 18, 1999.)